DTU Library

Indirect Wave Load Estimates Using Operational Modal Analysis
Preliminary Findings

Vigsø, Michael; Kristoffersen, Julie C.; Brincker, Rune; Georgakis, Christos T.

Published in:
Proceedings of the Twenty-eighth (2018) International Ocean and Polar Engineering Conference

Publication date:
2018

Document Version
Publisher's PDF, also known as Version of record

Citation (APA):
Vigsø, M., Kristoffersen, J. C., Brincker, R., & Georgakis, C. T. (2018). Indirect Wave Load Estimates Using Operational Modal Analysis: Preliminary Findings. In *Proceedings of the Twenty-eighth (2018) International Ocean and Polar Engineering Conference* (pp. 284-290). International Society of Offshore & Polar Engineers. Proceedings of the International Offshore and Polar Engineering Conference

Proceedings of the Twenty-eighth (2018) International Ocean and Polar Engineering Conference
Sapporo, Japan, June 10-15, 2018

ISBN 978-1-880653-87-6; ISSN 1098-6189
www.isope.org

Indirect Wave Load Estimates Using Operational Modal Analysis – Preliminary Findings

Michael Vigsø, Julie C. Kristoffersen*, Rune Brincker** and Christos T. Georgakis**
*Department of Engineering, Aarhus University, Denmark.
**Department of Civil Engineering, Technical University of Denmark, Kgs. Lyngby, Denmark

ABSTRACT

Wave loading on offshore structures has proven difficult to quantify through direct full-scale measurements. Therefore, engineers rely on codes and guidelines, numerical simulations, and scaled experiments in the design and as-built evaluation process. In this paper, it is shown that by monitoring the response of the structure and utilizing Operational Modal Analysis (OMA) it is possible to indirectly identify loads, occurring in actual conditions. A method employing modal parameters to establish a response function, which is used to back-calculate the hydrodynamic wave loading of a structure is presented. The process of inverting the system matrices is stabilized by merging the model with linear wave theory and hence constraining the solution to a scaling function of a predefined load distribution. The method is validated through a numerical case study and by wave flume experiments. Both cases are constituted as two-dimensional loading on a semi submerged cantilever cylinder.

KEYWORDS: Wave Loading; Indirect Measurements; Operational Modal Analysis; Offshore Structures

INTRODUCTION

In recent years concerning footage from the North Sea have been fuelling an intensive investigation lead by Mærsk. The recordings show plunging breaking waves at the Tyra field in close proximity to the offshore structures (Tychsen and Dixen, 2016). It was estimated that the wave heights were exceeding the 10 000 year return period for abnormal wave design. Questions have been raised whether the load effect of these extreme waves will compromise the reliability of the structures at sea.

Although much research has been done in the field of abnormal and breaking waves, it is evident that more research is needed in the field of extreme wave loading to offshore structures. Some issues remain elusive as most methods are based on scaled laboratory experiments. When conducting wave lab experiments, scaling effects will inevitable be present and especially in the case of breaking waves (Hughes, 2015).

A new approach - not subjected to scaling limitations for wave load quantification - is presented in this study. By monitoring the response of an offshore structure, the structure itself can be used as a live full scale load cell. This is done by inverse computations from the response of the structure. Limited research has been done specific to this application (Jensen et al., 1992; Perisic et al., 2014), whereas more focus has been given to indirect methods of e.g. fatigue assessment of offshore structures (Noppe et al., 2016; Maes et al., 2016). The indirect load identification of the wave action is a challenging discipline to verify, which may be the reason why little work has been done on this in the past. Input estimation in general is not a new topic as people have worked with this for many years.

In the late 80's Karl Stevens wrote an excellent overview on the topic of indirect load identification (Stevens, 1987). The paper outlines the challenges associated with this field of research, but also its potential. Many different approaches have since been tried out within the field of input identification. Most of the work done in this context are based on cases where the input is well defined and hence capable of verifying the results - either by using impact hammers or by simulation e.g. (Fritzen and Klinkov, 2014; Aenlle et al., 2007; Wang and Chiu, 2003). In resent years input identification using Kalman filters has proven successful (Lourens et al., 2012; Hwang et al., 2009; Naets et al., 2015; Liu et al., 2000; Maes et al., 2017).

In this paper, Operational Modal Analysis (OMA) will be used as a tool for modal identification of the structures in as-build conditions. The result from the OMA is used to make a model representation and this will be the key in deciphering the vibrations of the structure and hence estimate the wave loading.

The mathematical notation used is denoting matrices by a double underline and vectors by a single underline. Superscript* is a complex conjugate and superscript^T is a transposing operation.

THEORY

The response of a linear dynamic system, $\underline{y}(t)$, is defined as the convolution integral between the impulse response function, $\underline{\underline{h}}(t)$ and the a time varying load. (Brandt, 2011). The principle of load identification is to measure the response and then de-convolute this expression.

$$\underline{y}(t) = \underline{\underline{h}}(t) * \underline{f}(t) \triangleq \int_{-\infty}^{\infty} \underline{\underline{h}}(\tau)\, \underline{f}(t-\tau)\, d\tau \tag{1}$$

This integral is more conveniently evaluated in the frequency domain, so by means of the Fourier transformation Eq. 1 becomes:

$$\underline{Y}(\omega) = \underline{\underline{H}}(\omega)\, \underline{F}(\omega) \tag{2}$$

here, $\underline{Y}(\omega)$ and $\underline{F}(\omega)$ contain the Fourier coefficients of the response- and load vectors respectively. $\underline{\underline{H}}(\omega)$ is referred to as the Frequency Response Function (FRF). The FRF matrix can be constructed from either mass-, damping- and stiffness matrices or from modal parameters, which will be the case for this paper.

$$\underline{\underline{H}}(\omega) = \sum_{r=1}^{N} \left(\frac{Q_r \underline{\psi_r} \cdot \underline{\psi_r}^T}{i\omega - \lambda_r} + \frac{Q_r^* \underline{\psi_r^*} \cdot \underline{\psi_r^*}^T}{i\omega - \lambda_r^*} \right) \tag{3}$$

where, $\underline{\psi_r}$ is the mode shape vector for mode r. Q_r is a mode shape scaling constant and λ_r is the complex pole. The parameters needed for the FRF matrix - mode shapes and poles - can be experimentally determined by utilizing the concepts of operational modal analysis. (Brincker and Ventura, 2015). This is done by monitoring the response caused from what may be assumed as random excitation. For instance, in the context of offshore structures: small crested random waves and a light breeze touching the topside. The ID algorithm of choice can be applied and the modal parameters can be extracted from the signal. Both time- and frequency domain techniques exists for this.

Once the FRF matrix is estimated and the response of the structure, $\underline{Y}(\omega)$, is measured, the load can be calculated. This yields a type of inverse computation, where the load indirectly can be determined from measuring the response. Although it seems simple, problems persist as Eq. 2 is sensitive to truncation errors so when inverting the FRF matrix, the load estimate quickly becomes erroneous and may appear as non-physical.

As it was demonstrated by Vigsø et al. (2018) - if the load distribution is known this can be utilized to constrain the solution and hence improve the load estimate. This is implemented by separating the load variable from Eq. 1, into a spacial distribution, $\underline{f_0}$, and scaling function, $g(t)$:

$$\underline{f}(t) = \underline{f_0}\, g(t) \tag{4}$$

when inserting this definition into Eq. 2 we have

$$\begin{aligned} \underline{Y}(\omega) &= \underline{\underline{H}}(\omega)\, \underline{F}(\omega) \\ &= \underline{\underline{H}}(\omega)\, \underline{f_0}\, G(\omega) \\ &= \underline{C}(\omega)\, G(\omega) \end{aligned} \tag{5}$$

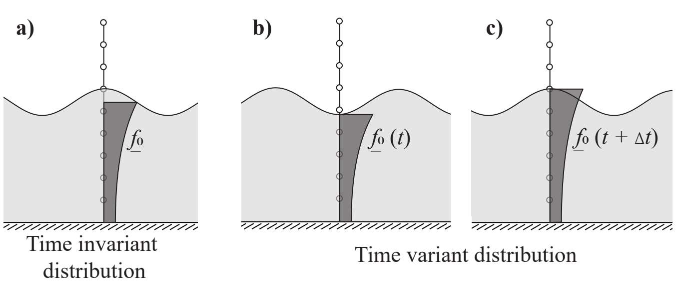

Fig. 1. Principle of spacial distributions, $\underline{f_0}$.

here, $\underline{C}(\omega)$ is the matrix product of the FRF matrix and the spacial distribution. The scaling function can now be estimated by a pseudo inverse operation.

$$\hat{G}(\omega) = \underline{C}^{\dagger}(\omega)\, \underline{Y}(\omega) \tag{6}$$

The final load estimate is then found by an inverse Fourier transformation and back substitution into Eq. 4. In order to do this, the spacial distribution, $\underline{f_0}$, must be known.

In order to apply this in the context of wave loading of an offshore structure it may be assumed that the structural loading is solely caused by water waves. Fig. 1 shows the principle of how the spacial distribution can be defined.

If the wave height is not recorded, the spacial distribution may be assumed as time invariant - for instance varying between the seabed and the mean water level as indicated by Fig. 1 **a)**. On the other hand - if the surface elevation is recorded simultaneously as the response of the structure, this additional information can be incorporated in the calculations, Fig. 1 **b)**, **c)**. For instance, taking the same distribution as in **a)** and stretching it to follow the surface elevation near the structure and hence assuming that the loading will occur at the entire wetted area.

When the spacial distribution of the load is changing in time (case **b)** and **c)**), the procedure for solving the scaling function changes. That is due to the convolution theorem which states that a product in the time domain is a convolution in the frequency domain and vice versa. If we apply the time variant definition of the spacial distribution, Eq. 2 becomes

$$\begin{aligned} \underline{Y}(\omega) &= \underline{\underline{H}}(\omega)\, \underline{F}(\omega) \\ &= \underline{\underline{H}}(\omega) \left(\underline{f_0}(\omega) * G(\omega) \right) && (7) \\ &= \underline{\underline{H}}(\omega) \int_{-\infty}^{\infty} \underline{f_0}(\xi)\, G(\omega - \xi)\, d\xi && (8) \end{aligned}$$

here, ξ is the frequency lag. As seen in the equation; when $\underline{f_0}(t)$ is a time variant function this yields a more complex problem to be solved. If the frequency content of the load is known this can be included else wise the equation can be solved through iteration.

SIMULATION

This simulation case study will demonstrate, that by monitoring the response of an offshore structure and applying the procedure described above, it is possible to indirectly estimate the wave load. A plane semi-submerged cantilever structure exposed to non-breaking waves will be the scope of this demonstration. The benefits of a simulation is that the method can be evaluated with as much noise as desired and the result

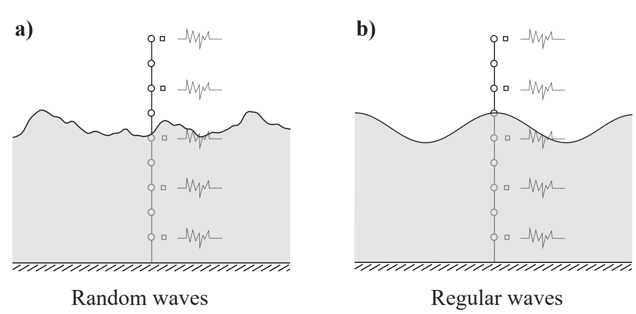

Fig. 2. Simulation sea states.

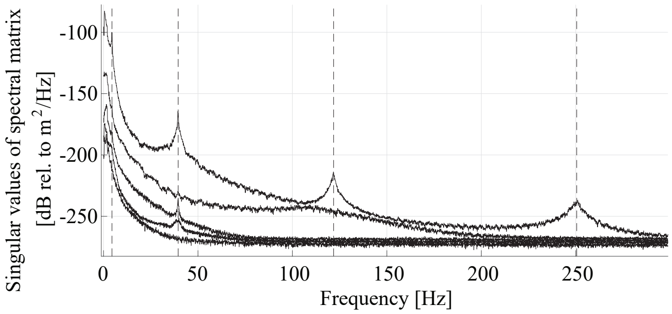

Fig. 3. Singular value decomposition of the response spectral density. Data composed using Welch averaging.

can be compared to the precise input and hence indicate how sensitive the solution is to different assumptions and sources of error.

The simulation is conducted as a plane scenario using an finite element (FE) cantilever beam model. The wave loading is evaluated using linear theory and Wheeler stretching to account for fluid motion above mean water level (Wheeler, 1969). Although fluid surrounding a structure is known to retard the response by added mass and damping, for this simulation, it is assumed that no interaction between the fluid and structure is present. The drag- and added mass coefficients are set to 1.3 and 1.9 respectively and the loads are evaluated using the Morison equation (Morison et al., 1950). (The coefficients are assumed to be unknown in the successive load identification). The geometrical quantities and hydrodynamic properties are selected to resemble the physical experiment covered by this paper (water depth 0.9 m, structure diameter 50 mm).

The simulation will be divided into two parts: 1): A simulation of the system response caused by a series of random waves. This shall be the basis for the OMA analysis and hence provide estimated modal parameters needed for the successive analysis of the wave loads. The random waves are synthesized from a Pierson–Moskowitz spectra with a peak frequency of 0.5 Hz and a significant wave height of 0.2 m.

2): Next a series with regular waves is simulated and shall be the basis for the indirect load identification calculations. A wave height of 0.2 m and period of 2 s is chosen as the sea state for the simulation. This gives a relative wave height of $H/h = 0.22$ and a wave steepness of $H/L = 0.04$. The two different simulation cases are shown by Fig. 2, where a set of five FE-DOFs are chosen as sensor information and only the response from these are kept for the analysis. The sensors in Fig. 2 are indicated by squares (□). For both of the simulation cases, a noise level of 150 dBW is added to the recorded signal.

Modal identification from random waves

The frequency domain response from 180 seconds of random wave simulation can be seen in Fig. 3 in terms of singular values (Brincker and Ventura, 2015). Despite the loading not being perfect white noise, four modes are revealed in the signal within the frequency band of 0-300 Hz. The modes are peak picked and analysed using the Frequency Domain Decomposition method (Brincker et al., 2000). The damping estimates are found by applying the Eigensystem Realization Algorithm (Juang and Pappa, 1985) at a band passed signal near the resonance frequencies. The modal parameters are listed in Table 1. Since no fluid/structure interaction is considered, the estimated modal parameters shall resemble the FE model with deviation only caused by noise and statistical error. The 4th mode shape from the FE model is an axial deformation mode and since only horizontal sensor information is available for the OMA, this mode cannot be estimated from the signal.

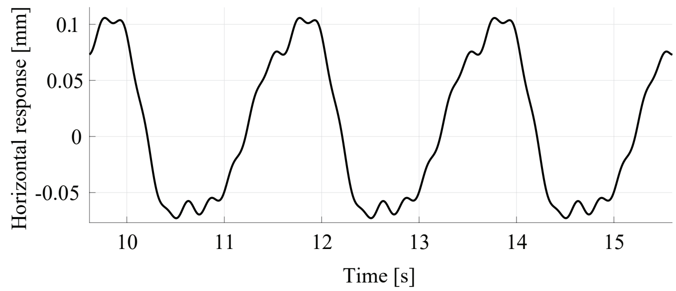

Fig. 4. Steady state response from top sensor when subjected to regular wave loading.

Table 1. Modal parameters from simulation case study.

FE model					
Mode	1	2	3	4	5
Natural Frequency, ω [Hz]	4.47	39.5	121	180	250
Damping Ratio, ζ [%]	1.80	0.33	0.45	0.61	0.82
OMA estimates					
Mode	1	2	3	4	5
Natural Frequency, ω [Hz]	4.46	39.5	122		251
Damping Ratio, ζ [%]	2.07	0.31	0.44		0.82

Assuming that the structural properties, geometry and material, are known quantities for the offshore structure. These can be used to make a new FE model to aid in the mass normalization of the OMA mode shapes. This FE model can also be used for mode shape expansion (O'Callahan et al., 1989) in order to obtain a higher resolution near the splash zone as desired. Now, the obtained modal parameters can be used to establish the frequency response function for the structure at actual in-place conditions, Eq. 3.

Load identification

The response due to regular wave loading is seen in Fig. 4. The response of the structure will be truncated in terms of the sensor position

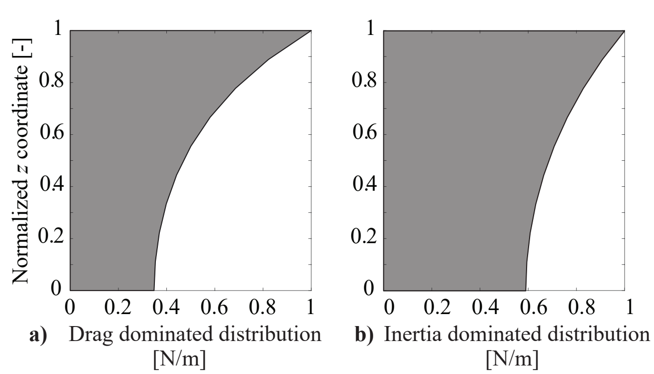

Fig. 5. Load distributions. **a)** Drag dominated is proportional to velocity squared. **b)** Inertia dominated is proportional to acceleration.

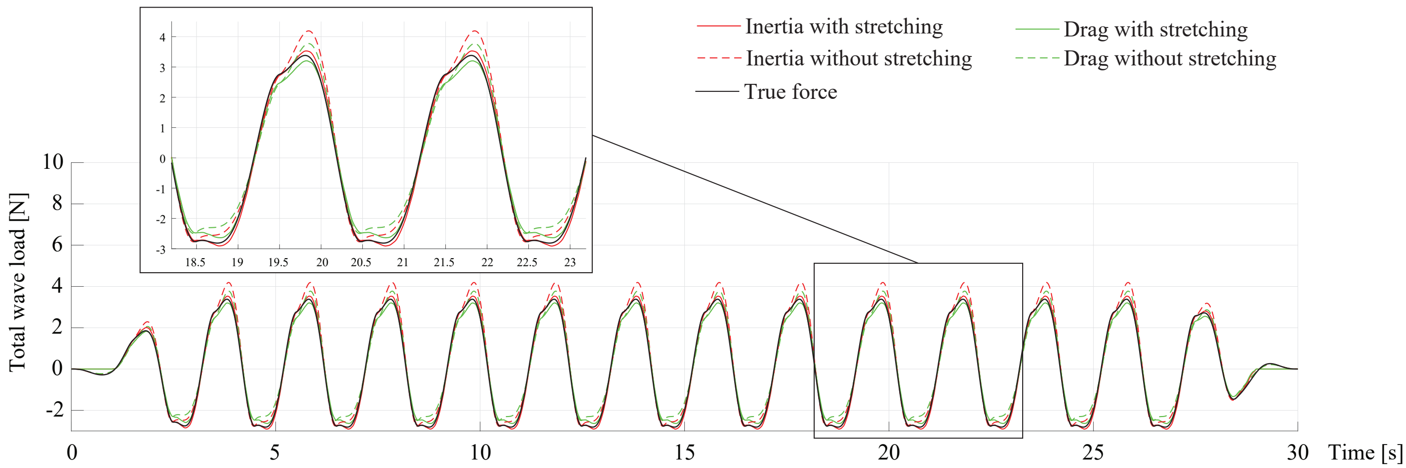

Fig. 6. Wave load estimate from the simulation case study. Both the time variant (with stretching) and time invariant (without stretching) solution are shown and compared to the actual input force in the simulation. The windowing is added during post processing.

and noise level though still be of value for the load identification.

Before making the final load identification calculation, the spacial distribution must be revisited. As the assumed load distribution is of great importance for the quality of the load estimate this must be selected with care. In principle any reasonable distribution can be used and for this study, two different distributions will be tried out. They are shown by Fig. 5. Distribution **a)** is generated from linear wave theory by assuming velocity squared proportionality at $du(z,t)/dt = 0$. Distribution **b)** is likewise generated from linear wave theory but from an acceleration proportional assumption at $u(z,t) = 0$. Information regarding water depth, wave height and period are of course needed to derive these. The normalized z coordinate is 0 at the seabed and 1 at the water surface. Both the distributions are normalized with a maximum value of 1 N/m. Neither of these will perfectly describe the actual loading used in the simulation, however it is demonstrated that they yield a reasonable approximation.

Fig. 6 shows the final load estimate for both the time variant and time invariant approach - recall their definitions from Fig. 1. The figure shows the total load applied to the structure from the wave action. As a general observation, for this type of cantilever structure, the assumed point of attack for the load distribution is governing for the load estimate. When the point of attack is assumed to be lower than the real, this will result in a over estimated load and vice versa. Hence the two time variant distributions (drag- or inertia dominated) will yield an absolute lower and upper bound for the estimate respectively and the span between should be considered as the uncertainty of the estimate.

If the surface elevation is not recorded - hence the distribution is described as time invariant - this yields an offset in the load estimate as the point of attack at some instances of time will be too low and at some instances too high. As seen from the estimates, the two solutions using stretching of the load distribution, yield a better estimate, than the time invariant distribution. It is expected that the deviation between the two methods will increase with the wave height.

EXPERIMENT

An experimental campaign has been conducted in a wave flume at Newcastle University, UK 2016 (Kristoffersen et al., 2018). A cantilever beam made from plexiglass is used for the experiment. The model is equipped with 7 uni-axial accelerometers; 6 positioned in the the wave direction and one in the transverse direction. Accelerometers used are Brüel & Kjær type 4508-B 100mV/g. Three wave gauges are positioned in line with the model and an average of these are used as a basis for the surface elevation, $\eta(t)$. The model and the sensor layout is sketched in Fig. 7.

The model is resting on a 6 DOF ATI load cell which is used to record the all the mudline forces. The mean water level of the flume is 0.9 m and the plexiglass model has a diameter of Ø50 mm. The total height of the model is 1.35 m.

Modal identification

As for the simulation case study; the model is observed at two stages, 1): Recording the response due to random excitation - the excitation is caused by making some random disturbance to the water surface surrounding the model. Again the concepts of OMA are deployed and mode shapes and damping estimates of the structure are obtained. For the frequency band of 0-100 Hz four in-plane bending modes were identified. Their frequency and damping ratio are listed in Table 2. The ID algorithm used is the same as for the simulation case study.

Disregarding the complex part of the mode shapes, an FE model is made and updated with focus on mode shape correlation and frequency match. The model is made using beam elements with 6 degrees of freedom (DOF) at each node. The influence of water is included as added mass below the mean water level.

As a simplification; proportional damping is assumed and coeffi-

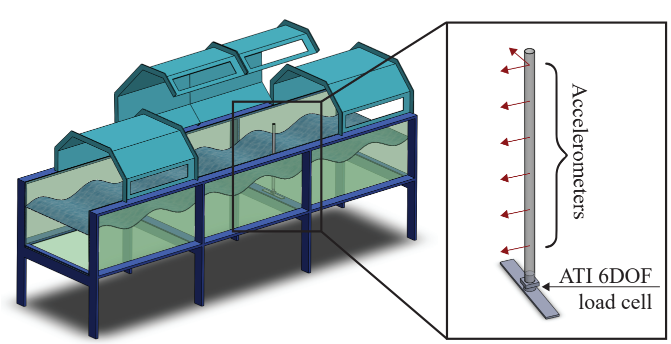

Fig. 7. Experimental setup.

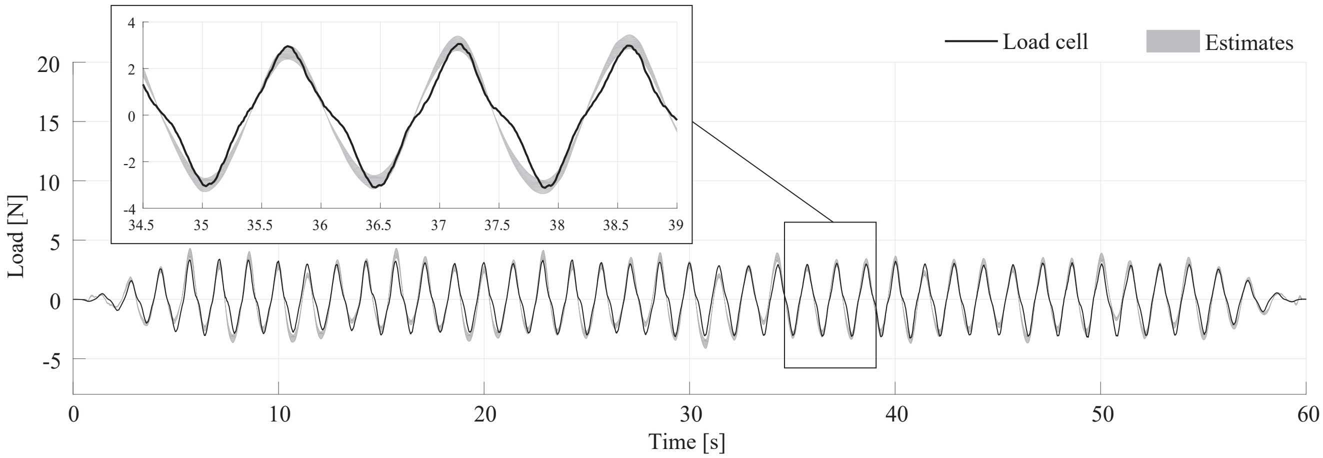

Fig. 8. Estimated total wave load from physical experiment. The shear force measured by the load cell is shown for reference. The windowing is added during post processing.

cients adjusted for a best fit. The FE model is used for mode shape expansion and mass normalization of the experimentally obtained mode shapes from the OMA analysis.

A frequency response function (FRF) of the system can yet again be formulated using Eq. 3. Obviously when using expanded mode shapes to construct the FRF matrix, the matrix will suffer from rank deficiency as no new modes are added. However, when the estimate is afterwards constrained by the assumed load distribution and solved by the pseudo inverse operation, this stabilizes the result.

Table 2. Modal parameters from experimental case study. (In-plane modes only).

OMA estimates				
Mode	1	2	3	4
Natural Frequency, ω [Hz]	2.12	13.4	44.5	97.7
Damping Ratio, ζ [%]	2.0	4.2	3.6	2.1

Load identification

2): Next step is to generate a wave configuration which can be used for the load computations. For this, a series of regular waves is chosen and the structural response is recorded. The waves are synthesized as linear waves with a period of 1.43 s and a wave height of 114 mm. These yield a relative wave height of $H/h = 0.127$ and a wave steepness of $H/L = 0.038$. The recording is initiated once the wave maker has reached a steady state output. As for the simulation case study; a set of two spacial distributions is used for the estimates. The distributions are generated in the same manner by assuming acceleration- or velocity proportionality and using linear wave theory. Only the solution using the time variant approach will be shown, i.e. utilizing the readings from the wave gauges and hence stretching the assumed load distribution to always cover the wet surface of the pile.

The solution on the load estimate can be seen in Fig. 8. The estimate is shown as an interval between the drag dominated and the inertia dominated distribution. From the same reasoning as mentioned earlier: the absolute lower bound is the drag dominated result and the absolute upper bound is the inertia result.

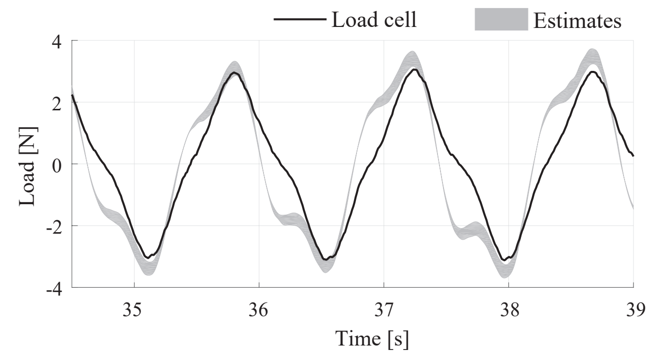

Fig. 9. Estimated dynamic reaction forces, shear.

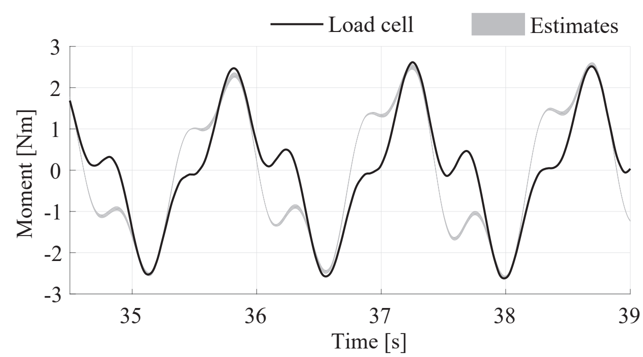

Fig. 10. Estimated dynamic reaction forces, moment.

In principle, now the wave load has been indirectly determined from the response. However, since the structure at hand has some dynamic properties, which yields a dynamic amplification to the wave loading, it is not possible to directly measure the wave load at the load cell and hence verify the estimates. The estimated load from Fig. 8 must then be transformed to reaction forces in order for a direct comparison to be made. Although accumulated uncertainty is present, this can be done by solving the unconstrained system of motion (Eq. 9), where the three response vectors are synthesized using the estimated load from Fig. 8 along with the mass, damping and stiffness matrices from the updated

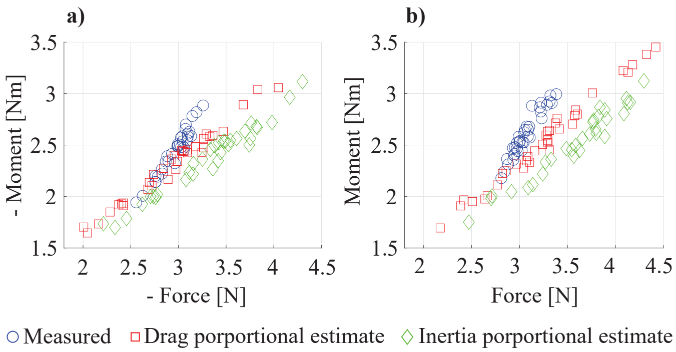

Fig. 11. Maximum mudline forces for each passing wave. Average relative wave height $H/h = 0.127$ and average wave steepness $H/L = 0.038$

FE-model.

$$\underline{\underline{M}}\,\underline{\ddot{y}}(t) + \underline{\underline{C}}\,\underline{\dot{y}}(t) + \underline{\underline{K}}\,\underline{y}(t) = \underline{f}(t) \tag{9}$$

here, $\underline{y}(t)$ is the nodal displacement, $\underline{\dot{y}}(t)$ is the nodal velocity and $\underline{\ddot{y}}(t)$ is the nodal acceleration.

The results of the estimated mudline forces (including dynamic amplification) are shown in Fig 9 and Fig. 10 along with the readings from the load cell. The measurements from the load cell are affiliated by a severe degree of noise from 50 Hz. Thus the measured values shown by Fig. 8 to 10 have been low-pass filtered at 40 Hz.

In terms of peak values for each passing wave, the estimated value of the force and moment is fairly good. Especially for the drag dominated end of the range. When it comes to variations between the peaks, the FE model is not capable in predicting the load variation and the estimate deviates more. This is naturally enough as the peak values of the load are the most governing for the response and as the response is the basis for the load estimate; the estimated load should have a best fit towards the peak values. The maximum and minimum forces and moments for each passing wave are plotted in Fig. 11. Fig. 11 **a)** shows the maximum negative forces i.e. caused during wave trough and Fig. 11 **b)** shows the maximum positive forces i.e. caused during wave crest. The mean value and standard deviations are given by Table 3 and 4.

From Fig. 11, linear wave theory adjusted by stretching of the profile seems to yield a too low point of attack - especially for the positive forces as indicated by Fig. 11 **b)**. As a result of that, the mean value of the estimated bending moments is in good agreement with the measurements, whereas the force is overestimated. The increase in standard deviation in the estimated values are suspected to originate from integration error and noise in the response measurements.

Table 3. Mean and standard deviation of the negative loads, i.e. from Fig 11 **a)**.

	Moment [Nm]		Force [N]	
	μ	σ	μ	σ
Measured	-2.44	0.22	-2.98	0.16
Drag proportional estimate	-2.31	0.53	-2.94	0.49
Inertia proportional estimate	-2.39	0.36	-3.36	0.56

Table 4. Mean and standard deviation of the positive loads, i.e. from Fig 11 **b)**.

	Moment [Nm]		Force [N]	
	μ	σ	μ	σ
Measured	2.60	0.22	3.07	0.15
Drag proportional estimate	2.54	0.44	3.26	0.55
Inertia proportional estimate	2.65	0.45	3.76	0.62

CONCLUSION

It has been demonstrated that operational modal analysis can be used for indirect load quantification for offshore structures. For the analyses presented, it has been assumed that the only loading to the structure is originated from wave action. If several other contributions are present this complicates the procedure. The paper also demonstrates that by merging different sensor information (accelerations and wave gauges/LIDAR) this can be incorporated in the load estimate. The method is not subjected to scaling issues and can be applied on a full scale if the response of the structure is successfully recorded and a well updated FE model is available.

Although the structures considered by this paper are based on a simple static systems, nothing dictates that the method cannot be applied on more complex systems as long as there are sufficient sensors to describe the additional mode shapes.

FUTURE WORK

Although the results presented by this paper are promising, they are based on a single structural system and one directional regular waves only. More research is needed in order to verify this method in cases where multi directional- irregular and even breaking waves are present.

ACKNOWLEDGEMENTS

The authors acknowledge the funding received from Centre for Oil and Gas – DTU/Danish Hydrocarbon Research and Technology Centre (DHRTC). Also the assistance provided by Bruna Silva Nabuco (Technical University of Denmark), during the experimental campaign in Newcastle needs to be acknowledged.

REFERENCES

Aenlle, M., Brincker, R., Fernández, P. and Fernández, A. (2007), ‘Load estimation from modal parameters’, *Proceedings of the International Operational Modal Analysis Conference, iomac* Vol. 1, pp 39–50.

Brandt, A. (2011), *Noise and Vibration Analysis*, Wiley.

Brincker, R. and Ventura, C. (2015), *Introduction to Operational Modal Analysis*, Wiley.

Brincker, R., Zhang, L. and Andersen, P. (2000), ‘Modal identification from ambient responses using frequency domain decomposition’, *Proceedings of the International Modal Analysis Conference, IMAC* pp. 625–630.

Fritzen, C. and Klinkov, M. (2014), ‘Load identification for structural health prognosis’, *NATO - Science and Technology Organization* .

Hughes, S. (2015), *Physical Models and Laboratory Techniques in Coastal Engineering*, World Scientific Publishing Co Pte Ltd.

Hwang, J., Kareem, A. and Kim, W. (2009), 'Estimation of modal loads using structural response', *Journal of Sound and Vibration* pp. 522–539.

Jensen, J., Kirkegaard, P. H. and Brincker, R. (1992), 'Modal and wave load identification by arma calibration', *Journal of engineering mechanics* .

Juang, J. and Pappa, R. (1985), 'An eigesystem realization algorithm for modal parameter identification and model reduction', *Journal of Guidance, Control, and Dynamics* 8, pp 620–627.

Kristoffersen, J., Georgakis, C., Bredmose, H. and Tao, L. (2018), 'Preliminary experimental study on the influence of the local wind field on forces from breaking waves on a circular cylinder', *ASME 37th International Conference on Ocean, Offshore and Arctic Engineering* .

Liu, J., Ma, C., Kung, I. and Lin, D. (2000), 'Input force estimation of a cantilever plate by using a system identification technique', *Comput. Methods Appl. Mech. Engrg.* pp. 1309–1322.

Lourens, E., Reynders, E., Roeck, G. D., Degrande, G. and Lombaert, G. (2012), 'An argumented Kalman filter for force identification in structural dynamics', *Mechanical Systems and Signal Processing* Vol. 27, pp 446–460.

Maes, K., Iliopoulos, A., Weijtjens, W., Devriendt, C. and Lombaert, G. (2016), 'Dynamic strain estimation for fatigue assessment of and offshore monopile wind turbine using filtering and modal expansion algorithms', *Mechanical Systems and Signal Processing* Vol: 76-77, 592–611.

Maes, K., Nimmen, K., Gillijns, S. and Lombaert, G. (2017), 'Validation of time-delayed recursive force identification in structural dynamics', *International Conference on Structural Dynamics, EURODYN* .

Morison, J., O'Brien, M., Johnson, J. and Schaaf, S. (1950), 'The force exerted by surface waves on piles', *Petroleum Transactions, American Institute of Mining Engineers* pp. 149–154.

Naets, F., Cuadrado, J. and Desmet, W. (2015), 'Stable force identification in structural dynamics using Kalman filter and dummy-measurements', *Mechanical Systems and Signal Processing* pp. 235–248.

Noppe, N., Iliopoulos, A., Weijtjens, W. and Devriendt, C. (2016), 'Full load estimation of and offshore wind turbine based on SCADA and accelerometer data', *Journal of Physics* .

O'Callahan, J., Avitabile, P. and Riemer, R. (1989), 'System equivalent reduction expansion process', *Proceedings of the International Modal Analysis Conference, IMAC* .

Perisic, N., Kirkegaard, P. H. and Tygesen, U. (2014), 'Load identification of offshore platform for fatigue life estimation', *Structural Health Monitoring* Vol. 5, pp 99–109.

Stevens, K. (1987), 'Force identification problems - an overview', *Proceedings of the SEM Spring Conference on Experimental Mechanics* pp. 838–844.

Tychsen, J. and Dixen, M. (2016), 'Wave kinematics and hydrodynamic loads on intermediate water depth structures inferred from systematic model testing and field observations – tyra field extreme wave study 2013-15', *Offshore Structural Reliability Conference, OSRC* .

Vigsø, M., Tarpø, M., Hansen, J., Brincker, R. and Georgakis, C. (2018), 'Scenario based approach for load identification', *Proceedings of the International Modal Analysis Conference, IMAC* .

Wang, B. and Chiu, C. (2003), 'Determination of unknown impact force acting on a simply supported beam', *Mechanical Systems and Signal Processing* Vol. 17, No 3, pp 683–704.

Wheeler, J. (1969), 'Method for calculating forces produced by irregular waves.', *Offshore Technology Conference* Vol 1, pp I–83 – I–94.